CHIN.PHYS.LETT. Vol. 25, No. 5 (2008) 1734

Experimental Investigation of Influence of Interfacial Tension on Convection of Two-Layer Immiscible Liquid *

LI Lu-Jun(李陆军), DUAN Li(段俐)**, HU Liang(胡良), KANG Qi(康琦)

[1]*National Microgravity Laboratory, Institute of Mechanics, Chinese Academy of Sciences, Beijing 100080*

(Received 19 January 2008)

Bénard–Marangoni convections of two-layer fluids heated from the bottom are investigated experimentally with a particle imagine velocimetry. The flows are visualized from the side, and various velocity fields near the onset of convection, such as three-layer vortex convective patterns, are observed when the depth ratio varies in a wide range. A new classification of the convective patterns is proposed with more detail than in previous studies. The analysis of the results indicates that the interface tension greatly influences the motion intensities of the bottom and top layers. The dimensionless wave number increases with the Bond number when the motion in the top layer is not more intense than that in the bottom layer, which agrees with the theoretical prediction.

PACS: 47. 20. Bp, 47. 20. Dr

Thermal convection in a horizontal liquid with an interface heated from bottom has been investigated since Bénard's experiments.[1−5] It is well known that two different mechanisms are responsible for the appearance of the cellular convection when the temperature difference across the liquid is above a threshold. They are buoyancy (Rayleigh–Bénard convection) that dominates in relatively thick layers, and interfacial tension (Marangoni convection) that dominates in very thin layers. In some cases, both mechanisms are active, which is referred to as the Bénard–Marangoni convection. Buoyancy effect and interfacial tension effect are characterized separately by the Rayleigh number Ra and Marangoni number Ma. The relative importance of the two effects is characterized by Bond number Bo, which is independent of the temperature difference. When $Bo > 1$, the buoyancy effect is more important; when $Bo > 1$, the interfacial tension effect is more important. Ra, Ma and Bo are defined as

$$Ra = \frac{\alpha\rho g h^3 \Delta T}{\mu\kappa}, \quad Ma = \frac{\sigma h \Delta T}{\mu\kappa},$$
$$Bo = \frac{Ra}{Ma} = \frac{\alpha\rho g h^2}{\sigma},$$

where ρ, κ, α, μ, σ, g, and h are the density, thermal diffusivity, thermal expansion coefficient, dynamic viscosity, temperature coefficient of interfacial tension, magnitude of gravity, thickness of the liquid, respectively; ΔT is the temperature difference across the liquid.

Two different convective patterns, thermal coupling and mechanical coupling, have been discovered in a two-layer fluid dominated by buoyancy.[2] Their main difference is the sign of the vorticity. The vorticity takes the same sign on both sides of the interface in the thermally coupled case, while the opposite sense of circulation is seen in the mechanically coupled case.

For buoyancy convection of a two-layer system, when $Ra_r > 1$, the motion in the top layer is more intense than that in the bottom layer; when $Ra_r < 1$, the motion in the bottom layer is more intense than that in the top layer; when $Ra_r \approx 1$, the competition between buoyancy convections in both the layers induces oscillatory convections.[6−8] Here Ra_r is defined as

$$Ra_r = \frac{Ra_2}{Ra_1} = \frac{\alpha_2}{\alpha_1}\frac{h_2^3}{h_1^3}\frac{\Delta T_2}{\Delta T_1}\frac{\nu_1}{\nu_2}\frac{\kappa_1}{\kappa_2}, \quad h_r = \frac{h_2}{h_1},$$

where the subscripts 1 and 2 denote the bottom layer and the top layer; ΔT_1 and ΔT_2 are the temperature differences across the bottom layer and the top layer, respectively, which can be calculated using the so-called "conduction assumption".

There have been a number of experimental studies on Rayleigh–Bénard convection in two-layer liquid systems, but very few on Bénard–Marangoni convection.[9,10] Nepomnyashchy *et al.*[11,12] investigated the influence of buoyancy on Marangoni convection in a two-layer system and predicted the transition from pure Marangoni convection to pure buoyancy convection accompanied by a significant growth of the wave number. The influence of the depth ratio on the appearance and disappearance of oscillations has been studied by Juel *et al.*[9] The flows were visualized from the top-to-bottom direction using the shadowgraph in their experiments. There is a limitation for the shadowgraph to measure the two-layer system. The shadowgraph images can only provide the temperature plot of one layer with the motion being more intense than the other layer. However, in most cases that the convective intensities in two layers are close, the shadowgraph images reveal nothing. Meanwhile, the comparison between convections in two layers as

*Supported by the National Nature Science Foundation of China (10432060, 10672171).

** Email: duanli@imech.ac.cn

an important part of the problem cannot be carried out with the shadowgraph.

In this study, the flow is visualized from side with a particle imagine velocimetry (PIV). The measurements on the velocity field at different depth ratios indicate that the interface tension plays an important role in the Bénard–Marangoni convection of two-layer fluid. Motion intension between the bottom layer fluid and the top layer fluid are compared indirectly by their maximum velocity magnitude of convection. More details about the convection patterns are also obtained. The horizontal dimensions of the vortices are measured, in comparison with the previous works. The dimensionless wave number W in the bottom layer fluid is defined as $W = \pi h_1/L$, where L is the mean value of the horizontal scale of the vortices in the bottom layer.

The experiments are conducted in a rectangle cavity with the top lid. The horizontal cross section of the cell is 100 mm × 40 mm. The bottom plate is heated by the electro-thermo film from bottom. The top lid made of optical glass is cooled by the circulating water from the thermostatic bath. The fluctuation of the temperature difference ΔT across the two liquid layers is kept within ±0.04°C. More details about the setup were given in Ref. [13]. We took a 3 M Fluorinert electronic liquid FC70 and the silicon oil KF96-10CS made by Shin-Etsu Chemical Co., Ltd of JAPAN. The two liquids are transparent and immiscible. Silicone oil lies on FC70 because the density of the former is smaller than the latter. The interfacial tension is assumed to decrease linearly with temperature at the interface and the temperature coefficient of interfacial tension σ is -4.46×10^{-5} N m^{-1} °C^{-1}. Their material thermo physical properties relevant to Bénard–Marangoni convections are listed in Table 1.

Table 1. Physical properties of the FC70 and the KF96-10.

		KF96-10	FC70
Density (kg·m^{-3})	ρ	935	1.93×10^3
Thermal conductivity (W·m^{-1}·K^{-1})	χ	0.134	6.9×10^{-2}
Thermal diffusivity (m^2·s^{-1})	κ	9.5×10^{-8}	3.48×10^{-8}
Thermal expansion (K^{-1})	α	1.1×10^{-3}	1.0×10^{-3}
Hydrodynamic viscosity (kg·m^{-1}·s^{-1})	μ	9.35×10^{-3}	2.702×10^{-2}
Kinematic viscosity (m^2·s^{-1})	ν	1×10^{-5}	1.4×10^{-5}

In our experiments, the total depth h remains constant, where $h = 8.56$ mm. As the depth ratio h_r varies in a wide range (0.25–6.35), five types of convective patterns near onset of convection are observed. The detailed classification is suggested by comparing the motion intensities in both the layers of one figure and considering the structure of the velocity field. The motion intensity is expressed by the magnitude of the velocity. The structure of the velocity field is expressed by the distribution and the shape of the vortices.

For $h_r < 1$, the motion is mechanically coupled convection I. The main feature of this type is the motion in the bottom layer is much more intense than that in the top layer besides the corresponding vortices in the bottom and top layers rotating in opposite directions. Figure 1 displays the velocity field of the system with the depth ratio h_r of 0.84 when the temperature difference is 2.33°C. With $Ra_r = 0.15$, the convective motion in the bottom layer is much more intense than the top layer. With $Bo_1 = 6.54 > 1$, the convection in the bottom layer is induced mostly by the buoyancy force. The horizontal scale of the convective cell is about 4.1 mm, so the dimensionless wave number is 3.5. Very weak convective vortices of 1.5 mm in height are induced by the viscous and the interfacial tension stress only near the interface in the top layer. The corresponding vortices in both the layers rotate in opposite directions. The similar velocity field of the system with smallest depth ratio of 0.25, when the temperature difference is 0.80°C, is shown in Fig. 2.

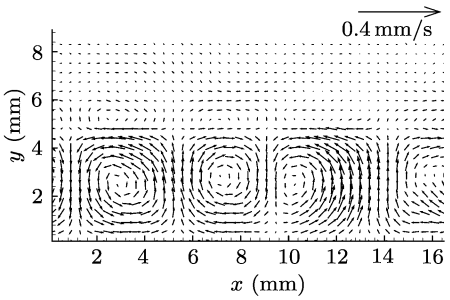

Fig. 1. Velocity field for $h = 8.56$ mm, $h_r = 0.84$, $\Delta T = 2.23$°C.

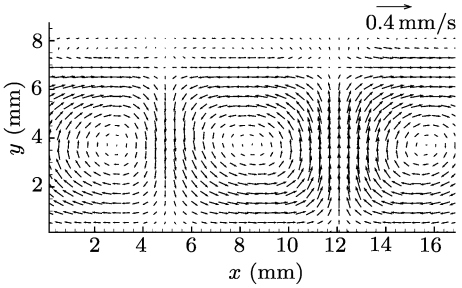

Fig. 2. Velocity field for $h = 8.56$ mm, $hr = 0.25$, $\Delta T = 0.8$°C.

For 1 $1 < h_r < 2$, the motion is mechanically coupled convection Ⅱ. The main feature of this type is that the convective motion near the interface in the top layer is slightly weaker than that in the bottom layer. The corresponding vortices in both the layers rotate in opposite directions. Except for the vortices near the interface, the top layer is nearly motionless. Similar phenomena are found in the numerical simulation. The velocity field of the system with depth ratio of 1.2, when the temperature difference is 2.46°C, is

shown in Fig. 3. With $Ra_r = 0.8$, the convective motion in the bottom layer is slightly more intense than that in the top layer. With $Bo_1 = 4.32$, the convection in the bottom layer is driven by the combination of buoyancy and interfacial tension stresses. The horizontal scale of the vortices in the bottom layer is about 4.5 mm, so the wave number is 2.6, which is near the value observed by Wayne *et al.*[10] The convection in the top layer is induced by the interfacial tension stresses and viscous forces which overcome buoyancy effect and heat diffusion effect. The interfacial tension stresses and the viscous forces induce a weak convective motion near the interface in the top layer. The vortices in the top layer of 2 mm in height are triangular in shape. The similar velocity field of the system with moderate depth ratio of 1.90, when the temperature difference is 3.15°C, is shown in Fig. 4.

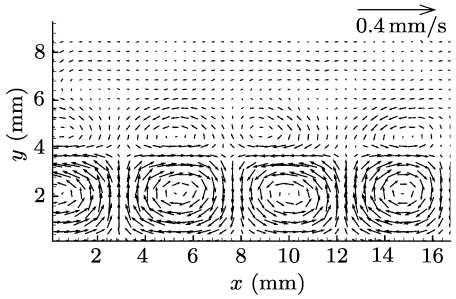

Fig. 3. Velocity field for $h = 8.56$ mm, $h_r = 1.27$, $\Delta T = 2.46$°C.

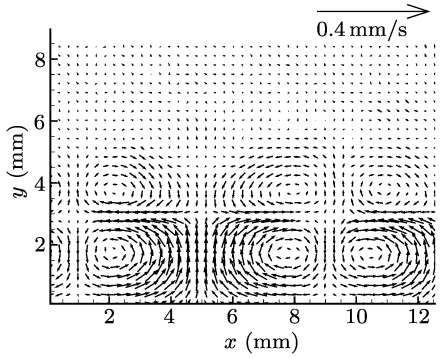

Fig. 4. Velocity field for $h = 8.56$ mm, $h_r = 1.90$, $\Delta T = 3.15$°C.

For $2 < h_r < 2.5$, the motion is oscillatory convection I. This type of convection is characterized by the feature that the intensities in both the layers are close and the flow structure is of three-layer vortices. The velocity field with the depth ratio of 2.34 is shown in Fig. 5. Although $Ra_r = 8.9 \gg 1$, the intensity of the bottom layer is comparable with the top layer because of the interfacial tension. With $Bo_1 = 1.99$, the convective vortices in the bottom layer is induced by the buoyancy and the interfacial tension. The horizontal scale of the vortices in the bottom layer is about 3.75 mm, so the dimensionless wave number is 2.1. With $Bo_2 = 8.14$, the buoyancy-driven convection is dominant in the top layer. The horizontal scale of the upper vortices in the top layer is twice that of the vortices in the bottom layer. The competition between the convections of the top and bottom layers causes the appearance of the vortices near the interface in the top layer of about 1 mm in height and with horizontal scale equal to that of the vortices of the bottom layer.

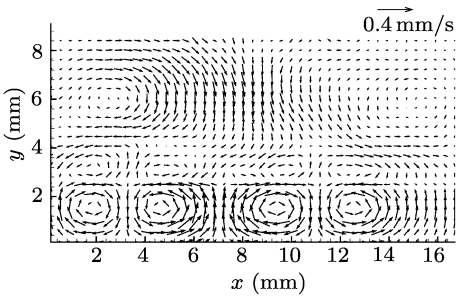

Fig. 5. Velocity field for $h = 8.56$ mm, $h_r = 2.34$, $\Delta T = 4.11$°C.

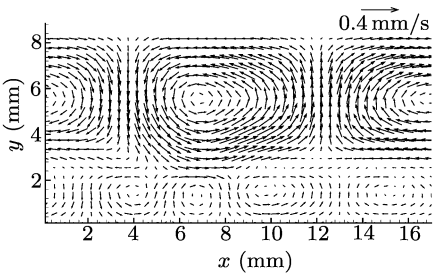

Fig. 6. Velocity field for $h = 8.56$ mm, $h_r = 2.64$, $\Delta T = 4.33$°C.

For $2.5 < h_r < 2.7$, the motion is oscillatory convection Ⅱ. The intensity of the motion in the bottom layer is weaker than that in the top layer and the horizontal scale of the vortices in the bottom layer varies in a wide range, which characterizes the oscillatory convection Ⅱ. Figure 6 shows the velocity field of the system with the depth ratio of 2.64. With $Ra_r = 14.4 > 1$, the motion in the top layer are more intense than that in the bottom layer. With $Bo_1 = 1.67$, the convection is induced jointly by the buoyancy and the interfacial tension. The horizontal scales of the vortices in the bottom layer vary in a wide range from 5 mm to 2 mm, so the dimensionless wave number varies from 1.5 to 3.75. With $Bo_2 = 8.72$, the convection is driven primarily by the buoyancy in the top layer. The horizontal scale of the vortices in the top layer is larger than that in the bottom layer. The flow directions near the interface in both the layers are the same at some places and opposite at other places. In related studies, the convection pattern with this feature is named the oscillatory convection.[14]

For $h_r > 2.7$, the motion is thermally coupled convection. The motion in the top layer is much more intense than that in the bottom layer, which charac-

terizes the thermally coupling convection. Figure 7 shows the velocity field of the system with the depth ratio of 4.01. With $Ra_r = 76.0$, the bottom layer is motionless compared with the top layer. On the one hand, for the bottom layer, the viscous stresses acting in the interface cannot overcome the buoyancy and the interfacial tension stress; on the other hand, the combination of the buoyancy and the interfacial tension can not overcome the viscous stresses and the heat diffusion effect. That explains the motionless in the bottom layer. With $Bo_2 = 10.61$, the convection in the top layer is dominated by the buoyancy force. Although the vortices are not observed in the bottom layer, the corresponding vortices in both the layers rotate in the same direction according to the theoretical prediction. Therefore, those convections are also named thermal coupling. The similar velocity field of the system with the largest depth ratio of 6.35 when the temperature difference is 2.03°C is shown in Fig. 8.

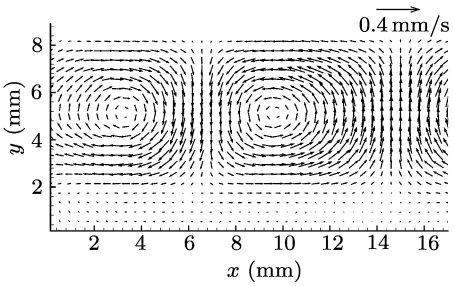

Fig. 7. Velocity field for $h = 8.56$ mm, $h_r = 4.01$, $\Delta T = 2.97$°C.

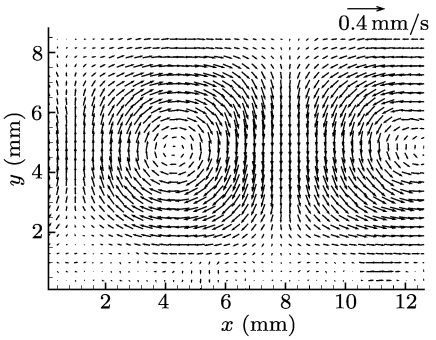

Fig. 8. Velocity field for $h = 8.56$ mm, $h_r = 6.35$, $\Delta T = 2.03$°C.

We also find that the dimensionless wave number w decreases with the local Bond number of the bottom layer Bo_1 when the motion in the top layer is not more intense than that in the bottom layer as shown in Fig. 9. The fact agrees with the prediction by Nepomnyashchy *et al.*[11] that the transition from the pure buoyancy convection to pure Marangoni convection is accompanied by the significant decrease of the wave number. With the depth ratio of 1.9, the dimensionless wave number w is 2.4, similar to the experimental value reported by Wayne *et al.*[10] and the theoretical prediction of Ferm *et al.*[15] As is known, a good result can be acquired with the shadowgraph method used by Wayne *et al.*[10] for $0 < h_r < 2$, where the motion in the bottom layer is more intense than the top layer; but for $2 < h_r < 2.5$ where the convective intensities in both layers are almost the same, good results cannot be obtained.

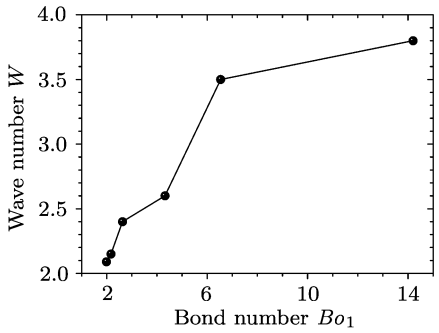

Fig. 9. Variation of wave number W with the local Bond number Bo_1 of the bottom layer.

In summary, as the total depth h is small ($h = 8.56$ mm) and the depth ratio varies in a wide range from 0.25 to 6.35, five types of convection patterns near onset are obtained with a PIV. The dimensionless wave number of the bottom layer, w, decreases with the local Bond number of the bottom layer Bo_1, in agreement with the theoretical prediction. Meanwhile, because of the Marangoni effect, the comparison between the intensities in the bottom and top layer can not be made by the criterion whether Ra_r is larger than 1 or not. The oscillatory region is expanded because of the interfacial tension which plays an important role in the Bénard–Marangoni convection of two-layer fluid.

References

[1] Bénard H 1900 *Rev. General Sci. Pure Appl.* **11** 1261
[2] Block M J 1956 *Nature* **178** 650
[3] Nield D A 1964 *J. Fluid. Mech.* **19** 341
[4] Pearson J R A 1958 *J. Fluid Mech.* **4** 489
[5] Rayleigh L 1916 *Philos. Magn.* **32** 529
[6] Prakash A, Otsubo F, Kuwahara K and Doi T 1997 *Exp. Fluids* **23** 252
[7] Degen M M, Colovas P W and Andereck C D 1998 *Phys. Rev.* E **57** 6647
[8] Renardy Y Y 1996 *Zeitschrift fur Angewandte Mathematik und Physik* **47** 567
[9] Anne J, John M, Burgess W D, McCormick J B and Swift H L 2000 *Phys.* D **143** 169
[10] Wayne A T et al 2000 *Phys. Rev. Lett.* **80** 3590
[11] Nepomnyashchy A A and Simanovskii I B 2003 *Phys. Rev.* E **68** 26301
[12] Nepomnyashchy A A and Simanovskii I B 2004 *Phys. Fluids* **16** 1127
[13] Li L J, Duan L, Hu L and Kang Q 2007 *Proceedings of The Seventh China National Conference On Experimental Fluid Mechanics* (Beidaihe, China 23–27 August 2007) p 88
[14] Colinet P and Legros J C 1994 *Phys. Fluids* **6** 2631
[15] Ferm E N and Wollkind D J 1982 *J. Non-Equilib. Thermodyn.* **7** 169